Water SA 52(3) 212–221 / Jul 2026
https://doi.org/10.17159/wsa/2026.v52.i3.4183

Research paper

Pollutant source identification in a Platinum Belt headwater catchment: a comparative geospatial assessment of dissolved and sediment-bound metals

Jonathan C Levin[1], Marc S Humphries[2], Christopher J Curtis[3] and Darragh J Woodford[1,4]

[1]*School of Animal, Plant and Environmental Sciences, University of the Witwatersrand, Johannesburg, South Africa*
[2]*School of Chemistry, University of the Witwatersrand, Johannesburg, South Africa*
[3]*School of Geography, Environmental Management and Energy Studies, University of Johannesburg, Johannesburg, South Africa*
[4]*South African Institute for Aquatic Biodiversity, Makhanda, South Africa*

Land-use stressors contribute to trace metal accumulation in aquatic ecosystems, yet South African river health assessments rely solely on dissolved metal monitoring, overlooking sediment analysis as a potential complement. The study objectives were to (i) monitor wet and dry seasonal variation in dissolved and sediment-bound Cr and Zn concentrations, (ii) identify at which spatial scale each sample type best predicts trace metal concentrations as a function of land-use and geology, and (iii) evaluate concordance between sample types across 14 sites in the Gwathle River catchment, South Africa. Using inductively coupled plasma mass spectrometry (ICP-MS) for water samples and energy dispersive X-ray fluorescence (EDXRF) for sediments, seasonal analyses revealed significantly higher dissolved Cr in the dry season, while no significant differences were observed for dissolved Zn. In addition, there were no significant seasonal differences in either sediment-bound Cr or Zn. Statistical modelling revealed that dissolved and sediment-bound Cr concentrations were best predicted by cumulative-scale mining impacts, while dissolved Zn correlated with sub-basin-scale lithology, and sediment Zn with combined urban and lithological factors. Spatial concordance analysis showed substantial agreement between water and sediment Cr signals along a land-use intensification gradient, indicating its conservative geochemistry enables effective multi-media source tracking. In contrast, Zn showed negligible phase concordance, suggesting dissimilar dissolved versus sediment-bound behaviour. The strong performance of Cr across both media demonstrates that paired sampling comprehensively traces pollution along intensification gradients. As a complementary tool for monitoring trace metals in South African aquatic ecosystems, sediment analysis may offer a pragmatic screening approach for assessing metal contamination across catchments, particularly where capacity constraints exist. This approach enables rapid and cost-effective delineation of persistent catchment contamination and profiling of metal distribution patterns across large areas, providing valuable insights for water resource management.

CORRESPONDENCE
Jonathan C Levin

EMAIL
jonathan.c.levin@gmail.com

DATES
Received: 3 December 2024
Accepted: 11 June 2026

KEYWORDS
trace metal monitoring
Bushveld Igneous Complex
multi-spatial scale assessment
multi-media sampling
water–sediment concordance

COPYRIGHT
© The Author(s)
Published under a Creative Commons Attribution 4.0 International Licence (CC BY 4.0)

INTRODUCTION

Ecosystems and societies alike depend on headwater streams for the provision of clean water. However, the integrity of these systems experiences a multitude of threats from the inputs of nutrients, sediments, organic and inorganic chemicals that degrade river water quality worldwide (Vörösmarty et al., 2010). Among the inorganic chemical contaminants, trace metals constitute a major hazard to global freshwater quality (Kolarova and Napiórkowski, 2021). Recent investigations have reported an alarming rise in aquatic metal pollution in South African rivers, attributing this increase to multiple stressors (Du Plessis and Curtis, 2021; Erasmus et al., 2022). The non-degradable and persistent nature of metals in water and riverine sediments threatens ecosystem integrity due to food web biomagnification (Amundsen et al., 1997). Prolonged trace metal exposure to aquatic organisms can damage organs, disrupt metabolic functions, and impair aquatic ecosystem functionality, which not only have cascading effects downstream but also pose serious health risks to human populations relying on these water resources for consumption and livelihood (Singh and Kalamdhad, 2011; Addo-Bediako et al., 2018). Such trace metal pollution is thus a major challenge for freshwater resource management, governance, and policy (Erasmus et al., 2022; Balaram et al., 2023).

While high-order rivers generally experience a greater number of stressors, accumulating contaminants from larger catchments, headwater streams may be particularly susceptible to contamination due to their small surface-to-edge ratio (Siziba et al., 2021). This is especially true for streams within the South African Bushveld Igneous Complex (BIC), a region renowned for its naturally elevated concentrations of metals. The BIC contains approximately 80% of the global platinum group metal (PGM) deposits, and other metals are also enriched relative to average upper continental crust, such as chromium (22-fold enrichment) and zinc (3-fold enrichment) (Barnes and Maier, 2002; Almécija et al., 2017; Erasmus et al., 2022). Mining is a well-known source of Cr and Zn in rivers of the South African BIC, while other human activities can also contribute to elevated concentrations of these metals in river systems (Barnes and Maier, 2002; Erasmus et al., 2022; Curtis et al., 2024).

Activities such as agriculture can contribute to elevated Zn concentrations in river systems, where the application of Zn-containing fertilizers, supplements, and protection products (e.g., fungicides) can run off into streams (Addo-Bediako et al., 2018). Urban settlements aided by stormwater infrastructure can also contribute elevated Zn concentrations, through automotive vehicles, galvanized roofing, and solid waste management as well as domestic sewage discharges (Addo-Bediako et al., 2018; Iloms et al., 2020).

Identifying key metal pollution sources in an area with already higher than natural background levels can assist resource managers to elucidate with greater specificity the contributing stressor sources and anthropogenic pathways of contaminants into headwaters to guide targeted mitigation efforts, thereby mitigating aquatic ecosystem and human-related impact (Albuquerque et al., 2022; Laha et al., 2022; Balaram et al., 2023). The complex topography, small size, and limited accessibility of local headwater streams, however, make regular monitoring challenging, hindering the collection of consistent spatio-temporal data necessary for identifying pollution sources and enabling adaptive catchment management.

Sediment and water sampling offer complementary approaches for monitoring metal pollution in aquatic ecosystems. While water sampling is widely employed in South Africa's Water Resource Quality Monitoring (WRQM) programme, this provides a snapshot of dissolved metal concentrations at the time of sampling and is subject to fluctuations due to flow conditions (DWAF, 2004; Bridgestock et al., 2022). In contrast, sediments can serve as time-integrated reservoirs of metal contamination in the landscape due to the sorption and binding affinity of trace metals to river particulates (Förstner and Müller, 1981; Devesa-Rey et al., 2010; Ciszewski and Grygar, 2016). While South African river health programmes currently lack sediment monitoring (DWS, 2016), rapid and relatively inexpensive analytical techniques, such as energy dispersive X-ray fluorescence (EDXRF), offer a promising tool to link sediment trace metal pollution to stressors (Laha et al., 2022). The choice between water and sediment samples for identifying transient versus residual sources of metal pollution will likely depend on the spatial scale of the stressors assessed relative to the study site. Natural ecohydrological controls on metal transport can be modified by catchment-scale human activities, influencing the spatial variability of dissolved and sediment-bound metal signals (Förstner and Müller, 1981; Shen et al., 2015; Bridgestock et al., 2022). A multi-spatial scale assessment is essential to investigate potential agreement between these sample media and to determine the relative meaningfulness of each for monitoring metal pollution in aquatic ecosystems.

This study aimed to track the movement of two key metal pollutants, Cr and Zn, in their dissolved and sediment-bound forms, across the Gwathle River catchment in South Africa's North West Province. The specific objectives were to: (i) monitor wet and dry seasonal variation in dissolved and sediment-bound metal concentrations, (ii) identify at which spatial scale each sample type best predicts key trace metal concentrations as a function of land-use and geology, and (iii) evaluate concordance (agreement and consistency) between the sample types' parsimonious statistical model outputs. Meeting these objectives would elucidate the complementary strengths of the two sample types for discerning anthropogenic metal pollution sources. Furthermore, this study will provide insights into the implications for monitoring pollution in river systems, helping water resource managers identify suitable scenarios for employing each sample type or their combinations.

METHODOLOGY

Study area

The Gwathle River catchment (Quaternary Catchment A21K; upper extent: 25°52'01.8"S, 27°25'56.4"E; lower extent: 25°24'13.2"S, 27°33'30.9"E), with an elevation ranging from ~1 843 m to 986 m, is part of the larger Limpopo Water Management Area and drains the northern slopes of the Magaliesberg Mountain Range between the towns of Rustenburg and Mooinooi, in the North West Province, South Africa (Fig. 1). The catchment receives ~629 mm of rainfall per year on average, with the typical wet season being between November and March and the dry season between April and October (Funk et al., 2015). Three rivers drain the catchment, where two are third-order rivers, being the Sterkstroom (Sites STK1-7), draining to the west, and the Maretlwane (Sites MRT1-7) to the east, before forming a confluence to form the fourth-order Gwathle River, draining north into Roodekoppies Dam.

The catchment experiences a stepped progression of stressors from the pristine headwater reaches, beginning with commercial irrigated agriculture, followed by urban and informal settlements, chromium and platinum mining, as well as mine-associated industrial activities, including smelters (Fig. 1). The upland quartzitic and minor-shale reaches of the catchment (Fig. 2) are partially contained within the Magaliesberg Biosphere Reserve, an area designated for ecotourism and sustainable development under the UNESCO Man and Biosphere Programme (Pool-Stanvliet, 2013). The lowland reaches traverse the Western Lobe of the BIC, and in particular both the Merensky Reef and the Upper Group 1 and 2 layers, which together form the most continuous layer among the Complex and contain among the world's richest PGE deposits (Von Gruenewaldt et al., 1986).

The BIC provides ~75% of global platinum production and ~50% of global chromite production (Almécija et al., 2017). The Lower Group 6 (LG-6) layer in the Western Limb is the most exploited chromitite layer and has a Cr_2O_3 content of 46–47% (Von Gruenewaldt et al., 1986; Schürmann et al., 1998). In addition, chromium content of chromitite layers is known to decrease upwards (Schürmann et al., 1998; Nikonow et al., 2023). The mafic-ultramafic layered intrusion in the lowlands of the study area contains Gabbro and Norite rock layers interspersed with anorthosite bands, among other lithological units (Fig. 2).

Land-cover class (stressor) determination

The stressor (land-use) data for the study area were obtained from the 2020 South African National Land Cover dataset (SANLC; GeoTerraImage, 2021). This ~20 m resolution product was derived from Sentinel-2 satellite imagery using a robust classification approach, resulting in high accuracy (Kappa Index > 0.85). To characterise key catchment stressors, Level 1 land-use classes within the Gwathle catchment were reclassified into 3 aggregated stressor categories: (1) cultivated land (commercial and annual crops), (2) urban (residential, smallholdings and commercial areas), and (3) mining (extraction pits, as well as wet and dry tailings facilities). These aggregated stressor classes representing major catchment stressors were processed using ArcGIS 10.5 software. Thereafter, the class-level 'percentage of landscape' (PLAND) metric was derived with the computer software FRAGSTATS 4.2 (McGarigal et al., 2002), indicating each stressor's proportion at the respective hydrological spatial scales.

Spatial scale delineation

The spatial design of this study enabled stressor effects on the aquatic ecosystems to be assessed at a (i) sub-basin scale, as well as the (ii) cumulative basin scale. For the sub-basin scale, each basin's extent was defined by the location of its respective study site (outlet location) and that of the study site immediately upstream on the same river. The cumulative catchment extent for each study site was defined from the outlet location of each study site, thereby including the rivers entire upstream catchment area, resulting in a nested hierarchy with the downstream sites reflecting the sum of the upstream sub-basins. Each sub-basin and cumulative basin were delineated using the Spatial Analyst tools in ArcGIS 10.5. The reclassified landscape stressor layers from the SANLC were clipped to each of the new spatial layers (i.e. scales) using the ArcGIS Data Management Tool to obtain spatial scales containing the proportions of the different stressors. Lithostratigraphic geological data were obtained for each spatial scale using the South Africa 250k Litho-Chronostratigraphic layer in ArcGIS 10.5 (Council for Geoscience, 2017).

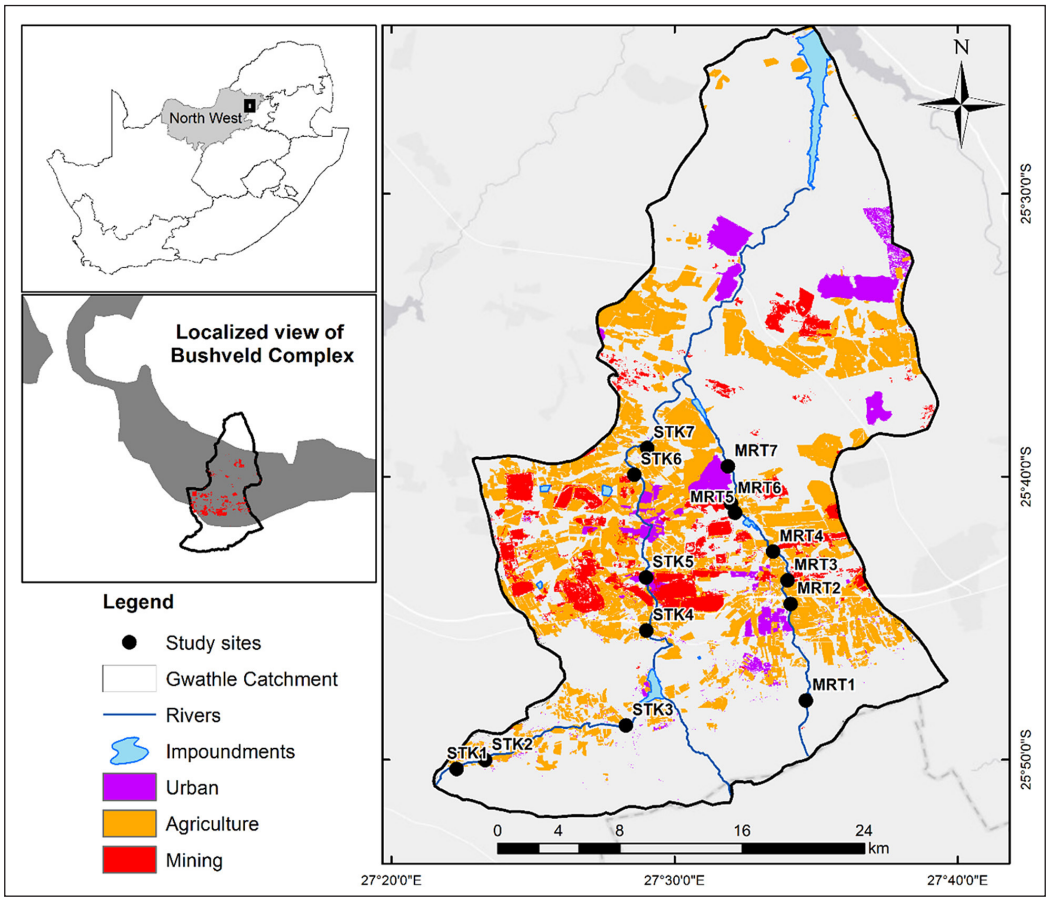

Figure 1. Map of the Gwathle study catchment within the Bushveld complex, as well as the sampling sites across the Sterkstroom (STK) and Maretlwane (MRT) rivers, draining an intensification gradient including natural (greyed area within), urban, agriculture and mining stressor activities.

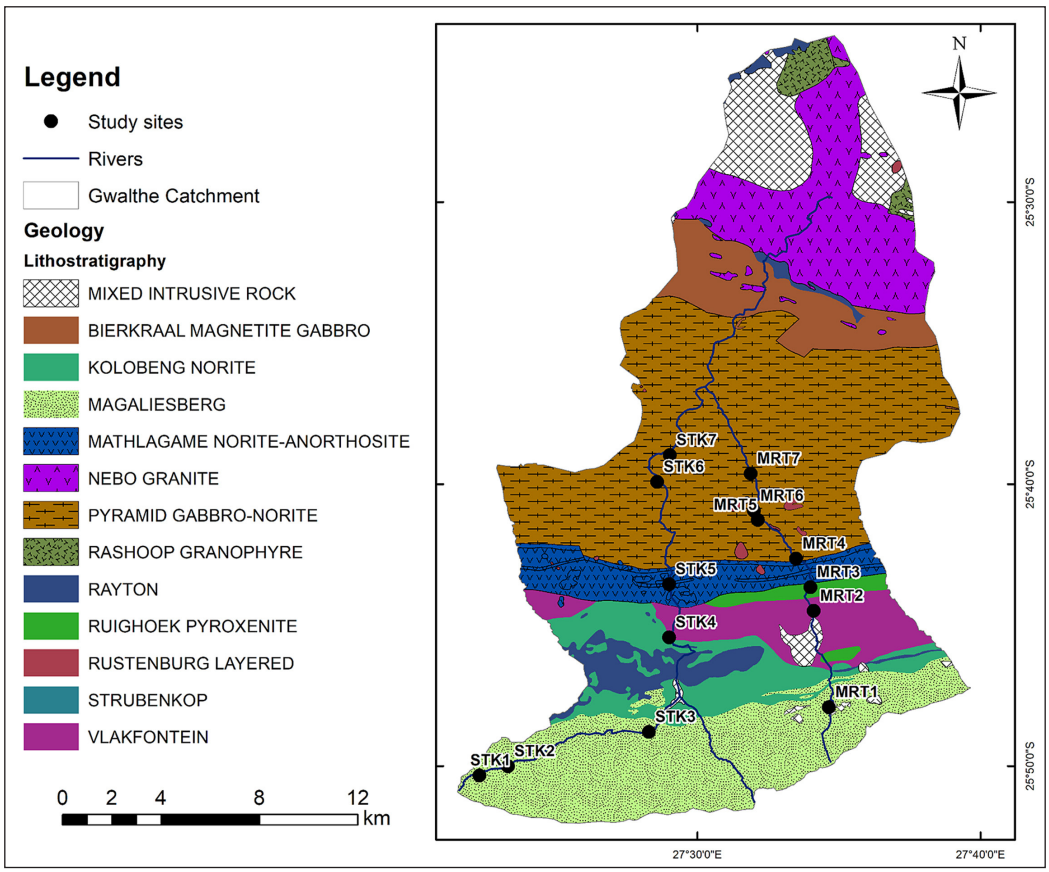

Figure 2. Map of the Gwathle study catchment geology (lithostratigraphy) with respect to the position of the Sterkstroom (STK) and Maretlwane (MRT) River study sites (Council for Geoscience, 2017). The main formations include Magaliesberg (part of the Transvaal sequence) quartzites and shales, as well as Pyramid Gabbro-Norite (part of the Rustenburg Layered Suite) composed of pyroxenite, Gabbro and Norite cumulative rock layers (Mitchell, 1990).

Sample collection and analysis

A total of 14 river sampling sites were established across the catchment, with 7 sites on the Sterkstroom River and 7 sites on the Maretlwane River, with the aim of capturing a range of natural and stressor variability, including informal–formal urban, agriculture and mining stressors in a stepped progression from upstream to downstream. At each site, samples were collected once during the wet season (April 2021) and once in the dry season (September 2021) (Table 1).

Water samples were collected 30 cm below the water surface at the thalweg of each site's active river channel. Samples were passed through Supor 0.45 µm filters and stored in 200 mL acid-rinsed polyethylene bottles. Samples were kept in cold storage and transported to the laboratory for further analysis. Analysis focused on Cr and Zn as these metals are found naturally enriched in BIC and represent common stressor pollutants associated with agriculture, urban, and mining activities in the region (Almécija et al., 2017). Metal concentrations were analysed using ICP-MS (Agilent 7800x), following calibration against a series of multi-element standard solutions. Analytical precision of replicate measurements (n = 5) was typically <5%. For sediment, 2 to 3 replicate samples were collected ~10 m apart (dependent on available sediments), to account for potential within-reach heterogeneity in grain size and varied depositional processes influencing metal accumulation at each sampling site. Sediment samples were collected from the top 5 cm of the river sediment using a square graduated plastic shovel, which best represents the recent surface deposition and greatest influence from potential stressor sources of heavy metals (Laha et al., 2022). The sediment replicates were collected and stored separately in unused labelled polyethylene plastic bags and stored frozen at –14°C until further laboratory processing.

In the laboratory, sediment samples were defrosted and wet sieved to <125 µm using deionized water. The <125 µm fraction was then air-dried for 24 h and homogenized into fine powder using a ball mill. Homogenized powders were placed into pre-weighed crucibles and combusted at ~550°C for 4 h to remove organic matter. Combusted powders were transferred to clean polyethylene sample cups and analysed for major oxides (SiO_2, Al_2O_3, $Fe2O_3$, CaO, K_2O, TiO_2) and selected trace elements (Cr and Zn) using a Bruker Ranger S2 EDXRF instrument. The instrument was calibrated using a range of USGS and local SARM rock standards. Measured concentrations were typically within 10% of accepted values.

To account for differences in sediment mineralogy and grain size between sites, metal enrichment factors (EF) were calculated using titanium oxide (TiO_2) as a conservative element. Samples collected from the two uppermost (pristine) river sites in the

Table 1. Study sites with their stressor descriptions at the two spatial scales assessed, as well as the dissolved and sediment-bound metal data collected over the wet and dry seasons

Study site	Latitude	Longitude	Possible pollution sources		Season	Dissolved metals		Sediment-bound metals	
			Sub-basin stressor(s)	Cumulative stressor(s)		Cr (ppb)	Zn (ppb)	Cr-EF	Zn-EF
STK1	–25.838786	27.37161	None	None	Wet	0.83	25.76	0.47	0.02
					Dry	0.84	24.65	0.48	0.01
STK2	–25.833387	27.388428	Agriculture	Agriculture	Wet	0.05	41.26	0.29	0.01
					Dry	0.98	31.87	0.24	0.01
STK3	–25.81307	27.47133	Agriculture	Agriculture	Wet	0.13	30.39	0.2	0.01
					Dry	0.98	44.5	0.25	0.01
STK4	–25.757205	27.483254	Agriculture	Agriculture	Wet	0.3	82.28	0.11	0.01
					Dry	0.98	43.82	0.13	0.01
STK5	–25.725874	27.483245	Mining	Agriculture, mining	Wet	1.09	61.54	2.4	0.01
					Dry	3.74	500.03	2.98	0.01
STK6	–25.665385	27.476215	Urban	Agriculture, mining, urban	Wet	1.02	36.47	0.56	0.01
					Dry	1.08	68.3	0.38	0.01
STK7	–25.649581	27.483748	Agriculture	Agriculture, mining, urban	Wet	1.03	90.44	0.21	0.01
					Dry	1.76	45.78	0.24	0.01
MRT1	–25.798461	27.577297	None	None	Wet	0.7	24.05	0.42	0.02
					Dry	0.94	28.57	0.45	0.02
MRT2	–25.741539	27.568359	Agriculture, Urban	Urban, agriculture	Wet	0.76	71.86	0.23	0.01
					Dry	0.92	38.99	0.32	0.02
MRT3	–25.727593	27.566446	Agriculture	Urban, agriculture	Wet	0.78	32.82	3.76	0.01
					Dry	1.4	65.28	2.67	0.01
MRT4	–25.710699	27.558002	Mining	Urban, agriculture, mining	Wet	7.66	118.1	7.05	0.02
					Dry	5.18	156.97	11.71	0.02
MRT5	–25.687824	27.535524	Mining	Urban, agriculture, mining	Wet	1.62	185.38	2.92	0.01
					Dry	4.59	384.03	3.95	0.01
MRT6	–25.682372	27.533205	Mining	Urban, agriculture, mining	Wet	Not sampled			
					Dry	11.83	878.09	8.47	0.02
MRT7	–25.660467	27.531345	Urban	Urban, agriculture, mining	Wet	4.61	376.96	1.8	0.01
					Dry	15.52	799.14	1.56	0.01

catchment were used to establish a local background reference value (Abrahim and Parker, 2008). The standardisation approach was achieved using the following equation:

$$EF = (metal/TiO_2)_{sample} / (metal/TiO_2)_{reference}$$

Statistical analysis

To assess the seasonal variability in trace metal concentrations between the wet and dry seasonal flows, one-way analysis of variance (ANOVA) tests were performed on generalized linear mixed effect models (GLMMs) for each technique-derived trace metal, with 'site' as a random effect. The GLMMs were constructed using the lme4 R package (Bates et al., 2015; R Core Team, 2023). A gamma distribution with log-link function was specified due to the positive, skewed distribution of trace metal data. To determine at which spatial scale each sample medium (water and sediment) best predicts trace metal concentrations as a function of land-use (i.e., capturing stressor effects) across the intensification gradient, the trace metal concentrations were modelled using GLMMs (Levin et al., 2024). Metal concentrations were modelled as a function of each stressor's proportion (%cultivated, %urban, %mining) at the respective spatial scale assessed. Geological type was added to account for potentially confounding lithostratigraphic factors, season as a fixed effect, and site as a random effect; all with additive terms.

Separate spatially explicit GLMMs were constructed at both sub-basin and cumulative basin scales for Cr and Zn from each sample medium (water and sediment), generating a total of 8 GLMMs. The most parsimonious model for each of the 8 GLMMs (the simplest model with the best fit) was sought using the dredge function from the MuMIn package (Bartoń, 2024). Comparing candidate parsimonious models for each media-derived metal at their respective spatial scales, the simplest yet most informative model was selected and retained based on the lowest Akaike's Information Criterion with small-sample correction (AICc) value. This thereby indicates the spatial scale at which the stress(ors) and/or confounding lithology best drives variation in each media-derived metal. This process resulted in 2 retained parsimonious models for each metal (i.e. one model retained per media at a spatial scale), resulting in 4 models in total being retained. The goodness-of-fit for the retained models was determined by the marginal R^2 ($R^2_{GLMM(m)}$; the variance explained for by the fixed factors) and the conditional R^2 ($R^2_{GLMM(c)}$; the variance explained by both fixed and random factors) coefficients using the r.squaredGLMM function in the MuMIn package (Wanderi et al., 2022).

To elucidate spatial trends (i.e., spatial detection patterns relative to stressor locations) and visualise agreement between the corresponding metals analysed via the two analytical techniques, predicted values (estimates of concentration and EF) from the parsimonious GLMMs were averaged across seasons and depicted on line graphs. Using the retained GLMM model predictions in visual and statistical analysis is advantageous, as it minimises the influence of confounding factors, as well as site-specific variability and differences in sampling seasons between sample types. This approach ultimately harmonises the data, enabling the comparison of estimated values from the two different analytical techniques along the river continua (Gelman and Hill, 2006).

Concordance correlation coefficient analysis (Lin, 1989) was performed to assess agreement and consistency quantitatively (evaluates congruence) between predicted values of the same metal derived from water versus sediment samples (unaveraged for each site). As a reproducibility index, the analysis provides information on both precision and accuracy to determine whether the two sample types produce consistent estimates of trace metal trends along the river continua. The concordance correlation coefficient (CCC) assesses correlation and bias, where $\rho = 1$ would indicate both techniques capture similar longitudinal trends ('almost perfect concordance'), while lower values suggest larger discrepancies (Landis and Koch, 1977). A bias correction factor (C_b) was reported, as it measures the deviation of the best-fit line from the ideal 45° line of perfect concordance, with values ranging from 0 to 1, where 1 indicates no deviation. The scale shift (v) indicates whether one method shows greater variability than the other, where a value of 1 indicates equal variability between the two methods (Lin, 1989).

RESULTS

Analysis of variance (ANOVA) on the dissolved metal GLMMs revealed significantly higher Cr in the dry season ($\chi^2 = 12.96$, $p < 0.01$), while no significant seasonal differences were recorded for Zn ($\chi^2 = 2.89$, $p = 0.09$); however, higher concentrations were recorded in the dry season. Analysis of variance on the sediment-bound metals GLMMs indicated no significant differences in standardised EF of Cr ($\chi^2 = 0.47$, $p = 0.49$) or Zn ($\chi^2 = 0.09$, $p = 0.77$) between seasons, although the dry season did record higher EF values in Cr (Table 1).

Following the GLMM analysis, 4 of the 8 models were retained based on best-fit, i.e., lowest AICc, and presented in Table 2. Model selection identified mining and a lithological unit as the most parsimonious predictors of increased dissolved Cr at the cumulative basin scale, while mining and lithology together best predicted increases in dissolved Zn at the sub-basin scale (Table 2). Among the predictive variables in the dissolved metal models, mining was the most important contributor in the Cr (cumulative basin scale) model, while lithology was the most important for the Zn (sub-basin scale) model (Table 3). The GLMM analysis for the sediment-bound metals identified that mining and lithology at the cumulative basin scale were associated with increased Cr, while urban stress and lithology also at the cumulative basin scale were associated with higher Zn (Table 2). The mining variable was also the most important predictor of sediment-bound Cr, whereas lithology was only negligibly higher than urban stress in predicting sediment-bound Zn (Table 3). The parameter estimates of each explanatory variable in the parsimonious models are presented in Table 3.

Line graphs generated from the predicted values of the retained parsimonious GLMMs (over the two seasons), indicated that the comparative trends for Cr between the two sample types across each river showed general agreement (Fig. 3). This is confirmed by the concordance correlation coefficient of $\rho = 0.67$ (95% CI: 0.40 to 0.83), indicating a substantial positive agreement, with uncertainty ranging from fair to almost perfect (Landis and Koch, 1977). The scale shift of $v = 0.92$ indicates near-equal variability between the dissolved and sediment-bound Cr predictions, suggesting that both sample types detected the Cr signal along the river continuum with almost equal consistency, from the pristine headwaters through to the mining-downstream sites. The bias-correction factor, C_b, of 0.98 indicates very minimal deviation on average from the best-fit line for the dissolved and sediment-bound metal predictions, and thus a good overall correlation.

There was a comparatively greater divergence between water and sediment Zn predicted values, with a noticeable separation of the trend lines (Fig. 3). The concordance correlation coefficient, $p = 0$ (95% CI: 0 to 0), confirms this, indicating no agreement between the two sample types. The scale shift $v = 0$ indicates that the dissolved Zn predictions showed no variability relative to the sediment-bound predictions, further supporting the absence of agreement between the two methods. The C_b of 0 indicates complete deviation from the best-fit line, rather than running parallel. Overall, the CCC analysis indicates very poor agreement between the Zn water and sediment models, with complete inconsistency, as opposed to the Cr water and sediment models, which presented substantial agreement.

Table 2. Four parsimonious generalized mixed effects models for each Cr and Zn response variables at the respective spatial scale they are best predicted at. Each model includes the model's explanatory stressor and geology. The (*) indicates the level of significance.

Sample type	Water (dissolved)		Sediment (benthic)	
Optimal scale	**Cumulative**	**Sub-basins**	**Cumulative**	
Response	**Cr**	**Zn**	**Cr**	**Zn**
Model predictors	• Mining • Vlakfontein	• Mining • Rayton • Ruighoek-Pyroxenite • Rustenburg layered	• Mining • Pyramid Gabbro-Norite	• Urban • Vlakfontein
Model intercept	−0.87(0.21)−4.16***	3.35(0.12)27.91***	−0.80(0.23)−3.49***	−3.71(0.06)−58.36***
		Model selection		
Weight	0.12	0.34	0.10	0.086
AICc	80.95	290.25	12.12	−214.25
BIC	84.5	293.4	13.66	−210.6
		Goodness of fit		
$R^2_{GLMM(m)}$	0.64	0.87	0.70	0.47
$R^2_{GLMM(c)}$	0.70	0.88	0.95	0.58
		Random effects		
Site (SD)	0.34	0.00	0.64	0.08
Residuals (SD)	0.49	0.39	0.28	0.15

Table 3. The conditional model parameter estimates for each variable in the parsimonious models, with the relative importance score for each variable. Greyed boxes indicating the variable with the greatest importance in the model, expressed as a rounded-up proportion.

Model spatial scale	Response	Variable	Variable estimate	Lower 95% CI	Upper 95% CI	Variable importance
Cumulative	Dissolved chromium	Mining	0.20	0.10	0.30	0.52
		Vlakfontein	0.04	0.01	0.07	0.48
Sub-basin	Dissolved zinc	Mining	0.09	0.07	0.11	0.21
		Rayton	0.05	0.03	0.07	0.21
		Ruighoek Pyroxenite	0.09	0.05	0.13	0.21
		Rustenburg Layered	0.62	0.45	0.80	0.36
Cumulative	Sediment chromium	Mining	0.64	0.61	1.16	0.59
		Pyramid Gabbro-Norite	0.28	0.37	0.18	0.41
	Sediment zinc	Urban	0.02	0.04	0.01	0.50
		Vlakfontein	0.03	0.00	0.01	0.50

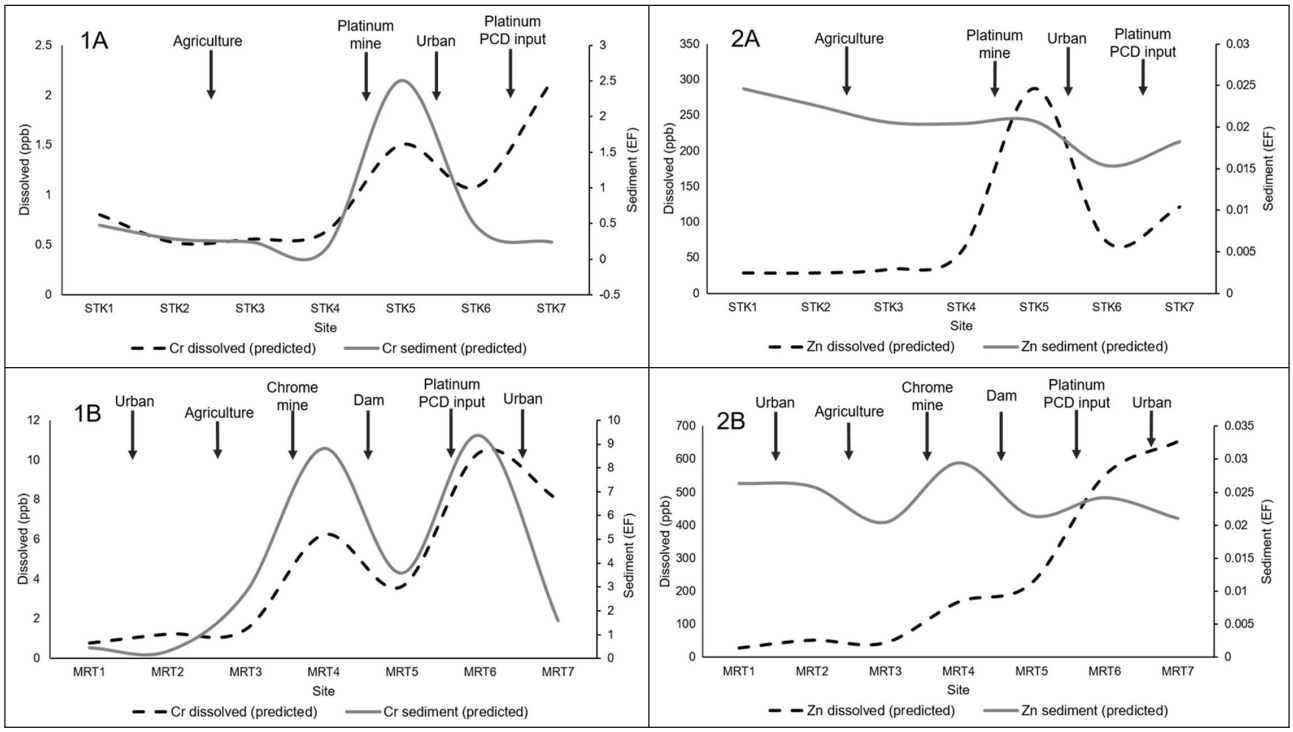

Figure 3. Comparative line graphs depicting predicted (estimated) Cr (1) and Zn (2) from the respective final parsimonious generalised linear mixed effects models from the water (black-dotted line) and sediment (grey-solid line) media along the (A) Sterkstroom (STK) and (B) Maretlwane (MRT) Rivers. Arrows indicate locations of known stressor introductions between sampling sites to enable visual assessment of coincident fluctuations in dissolved and sediment-bound metal concentrations.

DISCUSSION

Seasonal differences in water and sediment Cr and Zn

The contrasting seasonal variation between the metals analysed in water versus sediment provides insight into the environmental processes driving fluctuations in metal concentrations. For the dissolved metal analysis, Cr exhibited higher concentrations in the dry as opposed to the wet season, while Zn did not demonstrate significant seasonal variation. The high seasonal variation in Cr is supported by local literature (e.g., Dalu et al., 2017) and is driven by both changes in solubility and geochemical mobility of Cr between wet and dry hydrological conditions (Saalidong et al., 2022). During dry seasons, reduced flow volumes concentrate mining effluents, while also altering the geochemical conditions that affect Cr mobility and solubility. This is reflected in the higher recorded Cr levels during low flows compared to the wet season, where together with base flow, rainfall, and landscape runoff increase dilution (Almécija et al., 2017; Marara and Palamuleni, 2020).

The absence of a seasonal trend in dissolved Zn concentrations aligns with other investigations of mixed-use river catchments in South Africa (Edokpayi et al., 2016). This finding suggests a similar proportional pollutant input across the intensification gradient (Louis et al., 2014) and/or cyclic effects of eutrophication in the dry season (Jin et al., 2019; Sharma et al., 2022). While oxic conditions would favour Zn adsorption to Fe/Mn oxides in sediments during the wet season, this may not lead to a significant decrease overall in dissolved Zn concentrations, as the effectiveness of this process may be limited by high river flows. However, once adsorbed, Zn remains bound to sediments and is not released back into the water column (Jin et al., 2019; Sharma et al., 2022). Therefore, overall dissolved Zn concentrations may reflect a balance between dilution and adsorption processes.

Sediment-bound Cr and Zn concentrations revealed no significant difference between seasons, although Cr was marginally higher in the dry season compared to the wet season. During typical flow conditions, sediments can provide time-integrated signals of metal accumulation, though this pattern can be reset by high-flow scouring events. This temporal stability in sediment metal concentrations contrasts with water chemistry results, which reflect more immediate fluctuations in metal inputs.

Spatial scale influences and predictive drivers of dissolved metals

An assessment of the spatial scale at which trace metals from each sample type were best predicted revealed distinct patterns for the dissolved phase. Dissolved Cr displayed a broad, cumulative-scale accumulation pattern that was best predicted by a higher proportion of mining stress and lithogenic sources. Similar progressive Cr enrichment from mining activities has been observed in catchments with comparable stressor contexts, including the neighbouring Hex River catchment (Almécija et al., 2017) as well as in the Steelpoort River in Limpopo (Addo-Bediako et al., 2018). Among the predictive variables in the dissolved Cr model, mining was the most significant contributor to its variability (Table 3). Dissolved Zn, however, was best predicted by more localized sub-basin scale mining influences and various lithogenic sources, with the lithogenic sources contributing the greatest to the model (Table 3). The spatial scale dependency of the model for dissolved Cr and Zn may result from their respective inherent aqueous chemistries and associated transport pathways from systemic mining inputs and background erosional processes.

Among the model variables, percentage cumulative mining was the predominant predictor of increasing dissolved Cr, while the inclusion of the Vlakfontein lithology in the model may stem simply from spatial associations rather than direct mineralogical contributions and associated Cr release. For Zn, dissolved concentrations were best predicted at the sub-basin scale (between study sites), supporting its limited downstream transport potential, with local scale attenuation also observed by Gozzard et al. (2011) in a mining-stressed catchment. This suggests Zn^{2+} is readily removed via sorption during downstream transport, yielding a sub-basin scale signal that decays between the study sites within an otherwise nested study design.

Spatial scale influences and predictive drivers of metals in sediment

Unlike the spatial scale–dependent patterns observed in the dissolved models, the sediment-bound metal models showed cumulative-scale factors that best explained both Cr and Zn trends. The cumulative downstream accumulation of Cr in sediments is likely attributed to its stable complexation with metal oxyhydroxides (e.g., iron and manganese) and the lower mobility of Cr(III) forms (e.g., Richard and Bourg, 1991). Chromium likely enters the river systems from both background weathering processes (Almécija et al., 2017) and mining-related sources, including Cr-rich mineral (processed ore) and water (pollution control dam) effluents. Chromium was positively associated with a greater proportion of cumulative mining stress and a specific lithogenic source, Pyramid Gabbro-Norite (pyroxenite-gabbro-norite) (Table 2). Mines in the Western Lobe of the BIC largely exploit the Upper Group (e.g. UG-1 & UG-2; Cr_2O_3 = ~43%) and Middle Group reefs (including MG-1; Cr_2O_3 = ~46%) (Schürmann et al., 1998) of the Upper and Lower Critical Zones of the Rustenburg Layered Suite for chromium ores (Von Gruenewaldt et al., 1986). The Main Zone consisting of the Pyramid Gabbro-Norite unit is stratigraphically above these layers and lacks chromite but is extracted to access the deeper chromitites (Mitchell, 1990; Barnes and Maier, 2002). This supports its inclusion in the model and the rationale as to why the mining variable (as with dissolved Cr) remained the most important predictor for the Cr in sediment model at the cumulative scale (Table 3).

Sediment-bound Zn was positively associated with higher levels of urbanisation and the Vlakfontein lithology in the cumulative catchment. The similar contributions of these factors suggest that both predictors are nearly equally important in explaining the variability of instream sediment-bound Zn. Zinc exhibits a weak yet sufficient affinity for binding to sediment components to allow for a cumulative-scale retention capacity, as identified from the parsimonious Zn-sediment model (Table 2). The positive relationship between sediment-bound Zn and increased urban stress within the catchment (Table 3) is consistent with the findings of other studies (e.g., Louis et al., 2014; Dias-Ferreira et al., 2016). Such patterns may arise from Zn inputs from roofing materials, domestic wastewater effluents and other urban-related runoff, as well as the inherent geochemical attributes controlling its attenuation in the streambed (Louis et al., 2014).

Relationship between water and sediment samples

In comparing pollution signals between water and sediment, in the CCC analysis (Fig. 3), Cr displayed a substantial positive relationship (ρ = 0.67) between the analysed water and sediment media (Landis and Koch, 1977). This finding is supported by observations from the Steelpoort River, where both dissolved and sediment-bound Cr tracked a similar stressor gradient, with elevated concentrations at mining-impacted sites (Addo-Bediako et al., 2018). This may reflect processes such as the dominance of Cr(VI) species in the dissolved phase, which persists through anionic complexes, while particulate Cr(III) is stabilized through associations with mineral oxides (Richard and Bourg, 1991; Gorny et al., 2016). However, explicit investigation of speciation and phase

partitioning is still needed to substantiate the specific modes driving observed agreement for Cr across sediments and water within this catchment. The agreement between both sample types in relation to cumulative stressors indicates the capacity of both monitoring methods to detect broader river continuum pollution patterns.

In contrast, Zn showed negligible concordance between water and sediment, indicating no agreement between the two media (Fig. 3). This pattern is supported by observations from Addo-Bediako et al. (2018), who found that dissolved and sediment-bound Zn peaked at different sites relative to mining activities in the Steelpoort River. These findings suggest that Zn exhibits distinct behaviours in water and sediment, with differential phase partitioning and mobility. Unlike the dissolved phase, sediment-bound Zn exhibits a weak yet strong enough cumulative-scale retention capacity to integrate spatial pollution patterns. Consequently, the sediment-derived Zn trend better reflects spatial stressor dynamics along the two river continua compared to the aqueous-derived trend (Fig. 3).

Management implications

Currently, the analysis of dissolved metals is the primary monitoring approach used to assess metal pollution in South African national river health assessments. However, this study, focusing on Cr and Zn, suggests that incorporating routine sediment sampling could provide valuable long-term tracking of legacy metal pollution. While water sampling provides immediate snapshots of pollution levels and aids in short-term decision-making, its effectiveness is limited in stagnant river reaches (DWAF, 2004). Sediment-bound metal analysis can overcome such limitations, as it captures trace metal concentrations over time and space. This approach is particularly valuable in South Africa's extensive river networks, where logistical challenges often hinder frequent water sampling. By analysing sediments, long-term pollution trends and their connections to upstream sources within the catchment can be identified.

Sediment-bound metal analysis using EDXRF provides a practical, rapid, and cost-effective screening tool for profiling metal distributions. This approach enables large-scale assessments to identify hotspots, guide remediation, and evaluate cumulative impacts with limited sampling requirements. Combining sediment analysis with traditional water quality monitoring techniques can provide a more comprehensive assessment of South Africa's freshwater resources and help guide appropriate management strategies for achieving national water quality priorities (DWS, 2023). This study demonstrates the potential to develop national, affordable sediment monitoring protocols to identify sources of aquatic ecosystem stress. In the South African context, adding routine and cost-effective sediment metal analysis such as EDXRF could provide invaluable long-term pollution mapping to guide national water quality priorities and strategies.

CONCLUSION

This comparative geospatial assessment demonstrated that water and sediment sampling provided complementary approaches for tracking metal pollution from catchment stressors, with effectiveness dependent on metal geochemistry. Seasonal monitoring revealed significantly higher dissolved Cr in the dry season, while sediment-bound metals showed temporal stability, confirming their value as time-integrated indicators. Spatial scale analysis identified that dissolved and sediment-bound Cr were best predicted by cumulative-scale mining impacts, demonstrating conservative transport and progressive downstream accumulation, whereas dissolved Zn responded to sub-basin scale lithological controls and sediment-bound Zn to combined urban and lithological factors at the cumulative scale, reflecting its reactive geochemistry and rapid attenuation. Concordance analysis revealed strong agreement between water and sediment for Cr, indicating that paired sampling effectively tracks pollution along intensification gradients for conservative metals, while negligible concordance for Zn demonstrated metal-specific differences in environmental behaviour. While current South African water quality monitoring programmes emphasize 'snapshots' of dissolved concentrations, this study shows benthic sediments harbour valuable complementary signatures of mining-related stress. Sediment analysis via rapid techniques such as EDXRF offers a pragmatic, spatially integrated screening tool, given capacity constraints in national monitoring programmes, enabling rapid profiling of metal distribution across large areas to identify stressor impacts on conservative metals and inform water resource management.

ACKNOWLEDGEMENTS

Funding for this project was provided by the Water Research Commission of South Africa (Research contract C2019/2020-00153). JCL was supported by a DSI/NRF doctoral scholarship (MND210524603454). All fieldwork was conducted under a North West Province research permit (NW 17458/03/2020). The authors acknowledge the Environmental Geochemistry Laboratory in the School of Chemistry at the University of the Witwatersrand for the use of laboratory resources. The authors thank Dr Shaeen Chetty and Dr Letitia Pillay for assisting with laboratory quality control procedures. The authors thank Mark Ashfield and Gert Eastes for access to sampling sites on their properties.

AUTHOR CONTRIBUTIONS

Jonathan C Levin: data collection; data analysis, writing – original draft, review and editing, visualization, data validation; project administration; methodology; data curation, conceptualisation; and funding acquisition. Marc Humphries: writing – review & editing, laboratory access, and data validation. Christopher J. Curtis: writing – review & editing. Darragh J. Woodford: writing – review and editing, laboratory and field resources, project administration, funding acquisition.

ORCIDS

Jonathan C Levin
https://orcid.org/0000-0003-3839-2778

Marc S Humphries
https://orcid.org/0000-0002-4047-1451

Chris J Curtis
https://orcid.org/0000-0002-6597-2172

Darragh J Woodford
https://orcid.org/0000-0002-9460-5195

REFERENCES

ABRAHIM GMS and PARKER RJ (2008) Assessment of heavy metal enrichment factors and the degree of contamination in marine sediments from Tamaki Estuary, Auckland, New Zealand. *Environ. Monit. Assess.* **136** (1) 227–238. https://doi.org/10.1007/s10661-007-9678-2

ADDO-BEDIAKO A, MATLOU K and MAKUSHU E (2018) Heavy metal concentrations in water and sediment of the Steelpoort River, Olifants River System, South Africa. *Afr. J. Aquat. Sci.* **43** (4) 413–416. https://doi.org/10.2989/16085914.2018.1524745

ALBUQUERQUE PT, FREDOU T, BARCELLOS RL, MELO JT, ARRUDA GN and DE FRANÇA EJ (2022) Anthropogenic influences on sedimentary geochemistry of Itapessoca Estuarine Complex, Pernambuco, Brazil. *Environ. Monit. Assess.* **194** (1) 1–18. https://doi.org/10.1007/s10661-021-09699-3

ALMÉCIJA C, COBELO-GARCÍA A, WEPENER V and PREGO R (2017) Platinum group elements in stream sediments of mining zones: The Hex River (Bushveld Igneous Complex, South Africa). *J. Afr. Earth Sci.* **129** 934–943. https://doi.org/10.1016/j.jafrearsci.2017.02.002

AMUNDSEN PA, STALDVIK FJ, LUKIN AA, KASHULIN NA, POPOVA OA and RESHETNIKOV YS (1997) Heavy metal contamination in freshwater fish from the border region between Norway and Russia. *Sci. Total Environ.* **201** (3) 211–224. https://doi.org/10.1016/s0048-9697(97)84058-2

BALARAM V, COPIA L, KUMAR US, MILLER J and CHIDAMBARAM S (2023) Pollution of water resources and application of ICP-MS techniques for monitoring and management - a comprehensive review. *Geosyst. Geoenviron.* **2** (4) 1–24. https://doi.org/10.1016/j.geogeo.2023.100210

BARNES SJ and MAIER WD (2002) Platinum-group elements and microstructures of normal Merensky reef from Impala Platinum Mines, Bushveld Complex. *J. Petrol.* **43** (1) 103–128. https://doi.org/10.1093/petrology/43.1.103

BARTOŃ K (2024) Package 'MuMIn': Multi-model inference. R package version 1.48.4. URL: https://CRAN.R-project.org/package=MuMIn.

BATES D, MÄCHLER M, BOLKER B and WALKER S (2015) Fitting linear mixed-effects models using lme4. *J. Stat. Softw.* **67** (1) 1–48. https://doi.org/10.18637/jss.v067.i01

BRIDGESTOCK L, HENDERSON GM, HOLDSHIP P, KHAING AM, NAING TT, MYINT TA, HTUN WW, KHANT W, THU WM, CHI MAN and co-authors (2022) Dissolved trace element concentrations and fluxes in the Irrawaddy, Salween, Sittaung and Kaladan Rivers. *Sci. Total Environ.* **841** 1–13. https://doi.org/10.1016/j.scitotenv.2022.156756

CISZEWSKI D and GRYGAR TM (2016) A review of flood-related storage and remobilization of heavy metal pollutants in river systems. *Water Air Soil Pollut.* **227** 1–19. https://doi.org/10.1007/s11270-016-2934-8

COUNCIL FOR GEOSCIENCE (2017) South Africa 250k Litho-Chronostratigraphic layer (complete coverage). Council for Geoscience, Pretoria. URL: https://maps.geoscience.org.za.

CURTIS CJ, ROSE NL, YANG H, TURNER S, LANGERMAN K, FITCHETT J, MILNER A, KABBA A and SHILLAND J (2024) Contamination of depressional wetlands in the Mpumalanga Lake District of South Africa near a global emission hotspot. *Sci. Total Environ.* **938** 1–17. https://doi.org/10.1016/j.scitotenv.2024.173493

DALU T, WASSERMAN RJ, TONKIN JD, MWEDZI T, MAGORO ML and WEYL OL (2017) Water or sediment? Partitioning the role of water column and sediment chemistry as drivers of macroinvertebrate communities in an austral South African stream. *Sci. Total Environ.* **607** 317–325. https://doi.org/10.1016/j.scitotenv.2017.06.267

DEVESA-REY R, DÍAZ-FIERROS F and BARRAL MT (2010) Trace metals in river bed sediments: an assessment of their partitioning and bioavailability by using multivariate exploratory analysis. *J. Environ. Manage.* **91** (12) 2471–2477. https://doi.org/10.1016/j.jenvman.2010.06.024

DIAS-FERREIRA C, PATO RL, VAREJÃO JB, TAVARES AO and FERREIRA AJ (2016) Heavy metal and PCB spatial distribution pattern in sediments within an urban catchment – contribution of historical pollution sources. *J. Soils Sediments* **16** 2594–2605. https://doi.org/10.1007/s11368-016-1542-y

DU PLESSIS DM and CURTIS CJ (2021) Trace element contaminants associated with historic gold mining in sediments of dams and pans across Benoni, South Africa. *Environ. Monit. Assess.* **193** (122) 1–17. https://doi.org/10.1007/s10661-021-08854-0

DWAF (Department of Water Affairs and Forestry, South Africa) (2004) Water Resource Quality Monitoring Volume 1 – Sampling protocol for inorganic chemical analysis. Resource Quality Services, Department of Water Affairs, Pretoria, South Africa.

DWS (Department of Water and Sanitation, South Africa) (2016) River Eco-status Monitoring Programme. Department of Water and Sanitation. URL: http://www.dwa.gov.za/iwqs/rhp/rhp_background.aspx (Accessed 1 November 2025).

DWS (Department of Water and Sanitation, South Africa) (2023) National Water Resource Strategy. Third edition (NWRS-3). Department of Water and Sanitation, Pretoria.

EDOKPAYI JN, ODIYO JO, POPOOLA OE and MSAGATI TA (2016) Assessment of trace metals contamination of surface water and sediment: a case study of Mvudi River, South Africa. *Sustainability* **8** (2) 1–13. https://doi.org/10.3390/su8020135

ERASMUS JH, ZIMMERMANN S, SMIT NJ, MALHERBE W, NACHEV M, SURES B and WEPENER V (2022) Human health risks associated with consumption of fish contaminated with trace elements from intensive mining activities in a peri-urban region. *Sci. Total Environ.* **825** 1–12. https://doi.org/10.1016/j.scitotenv.2022.154011

FÖRSTNER U and MÜLLER G (1981) Concentrations of heavy metals and polycyclic aromatic hydrocarbons in river sediments: geochemical background, man's influence and environmental impact. *GeoJournal* **5** 417–432. https://doi.org/10.1007/bf02484715

FUNK C, PETERSON P, LANDSFELD M, PEDREROS D, VERDIN J, SHUKLA S, HUSAK G, ROWLAND J, HARRISON L, HOELL A and co-authors (2015) The climate hazards infrared precipitation with stations – a new environmental record for monitoring extremes. *Sci. Data* **2** (1) 1–21. https://doi.org/10.1038/sdata.2015.66

GELMAN A and HILL J (2006) *Data Analysis Using Regression and Multilevel/Hierarchical Models*. Cambridge University Press, Cambridge.

GEOTERRAIMAGE (2021) 2020 South Africa National Land-Cover Dataset. GeoTerraImage. URL: https://egis.environment.gov.za/sa_national_land_cover_datasets (Accessed 10 February 2022).

GORNY J, BILLON G, NOIRIEL C, DUMOULIN D, LESVEN L and MADÉ B (2016) Chromium behavior in aquatic environments: a review. *Environ. Rev.* **24** (4) 503–516. https://doi.org/10.1139/er-2016-0012

GOZZARD E, MAYES WM, POTTER HAB and JARVIS AP (2011) Seasonal and spatial variation of diffuse (non-point) source zinc pollution in a historically metal mined river catchment, UK. *Environ. Pollut.* **159** (10) 3113–3122. https://doi.org/10.1016/j.envpol.2011.02.010

ILOMS E, OLOLADE OO, OGOLA HJ and SELVARAJAN R (2020) Investigating industrial effluent impact on municipal wastewater treatment plant in Vaal, South Africa. *Int. J. Environ. Res. Public Health* **17** (3) 1–18. https://doi.org/10.3390/ijerph17031096

JIN Z, DING S, SUN Q, GAO S, FU Z, GONG M, LIN J, WANG D and WANG Y (2019) High resolution spatiotemporal sampling as a tool for comprehensive assessment of zinc mobility and pollution in sediments of a eutrophic lake. *J. Hazardous Mater.* **364** 182–191. https://doi.org/10.1016/j.jhazmat.2018.09.067

KOLAROVA N and NAPIÓRKOWSKI P (2021) Trace elements in aquatic environment. Origin, distribution, assessment and toxicity effect for the aquatic biota. *Ecohydrol. Hydrobiol.* **21** (4) 655–668. https://doi.org/10.1016/j.ecohyd.2021.02.002

LAHA F, GASHI F, FRANČIŠKOVIĆ-BILINSKI S, BILINSKI H and ÇADRAKU H (2022) Geospatial distribution of heavy metals in sediments of water sources in the Drini i Bardhë river basin (Kosovo) using XRF technique. *Sustain. Water Resour. Manage.* **8** (1) 1–16. https://doi.org/10.1007/s40899-022-00602-7

LANDIS JR and KOCH GG (1977) The measurement of observer agreement for categorical data. *Biometrics* **33** 159–174. https://doi.org/10.2307/2529310

LEVIN JC, CURTIS CJ and WOODFORD DJ (2024) A multi-spatial scale assessment of land-use stress on water quality in headwater streams in the Platinum Belt, South Africa. *Sci. Total Environ.* **927** 1–14. https://doi.org/10.2139/ssrn.4661528

LIN LI (1989) A concordance correlation coefficient to evaluate reproducibility. *Biometrics* **45** 255–268. https://doi.org/10.2307/2532051

LOUIS Y, PERNET-COUDRIER B and VARRAULT G (2014) Implications of effluent organic matter and its hydrophilic fraction on zinc (II) complexation in rivers under strong urban pressure: aromaticity as an inaccurate indicator of DOM–metal binding. *Sci. Total Environ.* **490** 830–837. https://doi.org/10.1016/j.scitotenv.2014.04.123

MARARA T and PALAMULENI LG (2020) A spatiotemporal analysis of water quality characteristics in the Klip River catchment, South Africa. *Environ. Monit. Assess.* **192** (9) 1–28. https://doi.org/10.1007/s10661-020-08441-9

MCGARIGAL K, CUSHMAN SA, NEEL MC and ENE E (2002) FRAGSTATS: Spatial pattern analysis program for categorical maps. Computer software, University of Massachusetts, Amherst. URL: https://www.fragstats.org/ (Accessed 20 January 2023).

MITCHELL AA (1990) The stratigraphy, petrography and mineralogy of the Main Zone of the northwestern Bushveld Complex. *S. Afr. J. Geol.* **93** (4) 818–831.

NIKONOW W, RAMMLMAIR D and MEIMA JA (2023) Continuous element mapping of drill cores from the Bushveld Complex, SA using LIBS and μEDXRF. *Soc. Geol. Appl. Miner. Deposits* 57–60. https://doi.org/10.5194/egusphere-egu23-16429

POOL-STANVLIET R (2013) A history of the UNESCO Man and the Biosphere Programme in South Africa. *S. Afr. J. Sci.* **109** (9) 1–6. https://doi.org/10.1590/sajs.2013/a0035

R CORE TEAM (2023) R: a language and environment for statistical computing. R Foundation for Statistical Computing, Vienna, Austria. URL: https://www.R-project.org.

RICHARD FC and BOURG AC (1991) Aqueous geochemistry of chromium: a review. *Water Res.* **25** (7) 807–816. https://doi.org/10.1016/0043-1354(91)90160-r

SAALIDONG BM, ARAM SA, OTU S and LARTEY PO (2022) Examining the dynamics of the relationship between water pH and other water quality parameters in ground and surface water systems. *PLoS ONE* **17** (1) 1–17. https://doi.org/10.1371/journal.pone.0262117

SCHÜRMANN LW, GRABE PJ and STEENKAMP CJ (1998) Chromium. In: Wilson MGC and Anhaeusser CR (eds) *Chromium Mineral Resources of South Africa: Handbook 16*. Council for Geoscience, Pretoria. 90–106.

SHARMA N, WANG Z, CATALANO JG and GIAMMAR DE (2022) Dynamic responses of trace metal bioaccessibility to fluctuating redox conditions in wetland soils and stream sediments. *ACS Earth Space Chem.* **6** (5) 1331–1344. https://doi.org/10.1021/acsearthspacechem.2c00031.s001

SHEN Z, HOU X, LI W, AINI G, CHEN L and GONG Y (2015) Impact of landscape pattern at multiple spatial scales on water quality: a case study in a typical urbanised watershed in China. *Ecol. Indic.* **48** 417–427. https://doi.org/10.1016/j.ecolind.2014.08.019

SINGH J and KALAMDHAD AS (2011) Effects of heavy metals on soil, plants, human health and aquatic life. *Int. J. Res. Chem. Environ.* **1** (2) 15–21.

SIZIBA N, MWEDZI T and MUISA N (2021) Assessment of nutrient enrichment and heavy metal pollution of headwater streams of Bulawayo, Zimbabwe. *Phys. Chem. Earth* **122** 1–8. https://doi.org/10.1016/j.pce.2020.102912

VON GRUENEWALDT G, HATTON CJ and MERKLE RKW (1986) Platinum-group element-chromitite associations in the Bushveld Complex. *Econ. Geol.* **81** (5) 1067–1079. https://doi.org/10.2113/gsecongeo.81.5.1067

VÖRÖSMARTY CJ, MCINTYRE PB, GESSNER MO, DUDGEON D, PRUSEVICH A, GREEN P, GLIDDEN S, BUNN SE, SULLIVAN CA, LIERMANN CR and co-authors (2010) Global threats to human water security and river biodiversity. *Nature* **467** 555–561. https://doi.org/10.1038/nature09440

WANDERI EW, GETTEL GM, SINGER GA and MASESE FO (2022) Drivers of water quality in Afromontane-savanna rivers. *Front. Environ. Sci.* **10** 1–20. https://doi.org/10.3389/fenvs.2022.972153